Fourier Methods for Turbomachinery

L. He
Department of Engineering Science,
University of Oxford,
Oxford, OX1 3PJ, United Kingdom

Abstract

Advanced turbomachinery development calls for efficient and accurate methods development. In a design cycle, large number flow solutions are sought to interact iteratively or concurrently with various options, opportunities and constraints from multiple disciplines. This basic requirement for fast prediction methods in a multi-disciplinary design environment remains unchanged, regardless of ever-increasing computer power. A general issue of interest in understanding and prediction of turbomachinery flows is: how do periodic unsteady disturbances affect time-averaged flow? Bear in mind that engine performance parameters are based on a time-averaged ('steady') flow state. Multi-disciplinary, often competing factors are also compared, ranked and accounted for on a common time-averaged ('steady') base state. In a fundamental sense, the situation is no different to how general turbulent (unsteady) disturbances affect time-average flows through nonlinearity-generated 'Reynolds Stresses'. Then, how should we treat turbomachinery unsteady flows, similarly to (or differently from) how turbulence has been treated?

It is against the background above that the Fourier methods have been developed for efficient nonlinear flow solutions to unsteady turbomachinery flows since 1990. The main impetus is to develop efficient and adequately accurate computational methodologies and working methods for prediction and analysis of the unsteady flow effects on aerothermal performance (loading and efficiency) and aeroelasticity (blade vibration due to flutter and forced response) in turbomachinery. This lecture provides an updated and extended overview based on a review paper on the subject (He 2010 [1]). We will start with a brief look at some major historic milestones in turbomachinery flow computations, underlining the motivation for the Fourier method development. We will then look at various forms of Fourier methods and implementations with their salient features contextually highlighted. Although the main emphasis has been on the temporal Fourier models (in time domain or frequency domain) where major efforts and progress have been made, the spatial Fourier modelling development is also described. Several computational case examples are given to illustrate validity and effectiveness of the corresponding methods respectively.

1. Background: Some Turbomachinery Context in 'Turbomachinery CFD'

Let's start with a seemingly simple question: how much 'Turbomachinery' is there in 'Turbomachinery CFD'? As the introduction, we will first look back on some key past development efforts and corresponding challenges in two related topic areas: Turbomachinery unsteady flow and Blade aeroelasticity. We will then have a brief account of the main Fourier method development in the past three decades or so, before moving to the other sections with more detailed descriptions, discussions and illustrative examples about the corresponding methods.

1.1. Aerodynamic Models: from Single-Passage to Multiple-Bladerows

At a fundamental level, a turbomachinery blade section is designed to function in a similar way to an aircraft wing section: to turn flow as much and as efficiently as it can. Complex three-dimensional as well as unsteady interactions in turbomachinery flows however do present distinctive challenges. Consequently, design considerations of flow turning and losses on a 2D blade-blade cascade section would not be nearly sufficient. It is thus not surprising that for very long time, the main working methodology for turbomachinery design has been based on the 'throughflow method'. A throughflow model working on a meridional (axial-radial) plane with some more mature and notable efforts by Smith 1966 [2], Marsh 1966 [3]. It deals with a circumferentially averaged flow on the meridional (axial-radial) plane. This basic feature of the throughflow methodology underlines the importance of the 'radial equilibrium' (blade spanwise interaction), without which any design intent flow turning on a 2D cascade section, as powerful and efficient as it might sound, may not be physically realizable. Nevertheless, a throughflow solution can only be reasonable if the input information of flow turning (loading) and losses on spanwise sections is reasonable. Thus a throughflow model on a meridional plane would have to interact with a cascade flow model on a spanwise section.

A major step towards describing 3D effects was put forward by Wu 1952 [4] to couple two 2D subsystems. One 2D subsystem is a set of stream surfaces similar to a cascade flow model (S1 surface). The other subsystem is a set of 2D stream surfaces similar to the throughflow model (S2 surface). The system solutions in principle should lead to a full 3D flow description. In practice, the coupling between the two stream surfaces could be quite complex given typical complex 3D flow patterns, particularly near end-walls.

The start of Turbomachinery CFD proper is marked by the pioneering work of Denton 1975 [5]. The multiple blade passages of the same geometry enable a circumferential truncation from the whole 360° annulus to a single blade passage domain. A single blade-passage domain becomes a basic unit of turbomachinery flow, which has been used as a starting point almost invariably in all the prediction and analysis methods for conventional turbomachinery flow designs. Furthermore, the use of a relative frame of reference would enable most prevalent flow mechanisms to be captured to a large extent by a steady flow model. It is this basic single-passage steady flow model that has dominated the turbomachinery flow analyses in a design environment for the past 50 years. Significant advancement in predictability and understanding of 3D flows in blade passages has been brought about since Denton's landmark paper in 1975. The flow modelling fidelity had been improved from an inviscid Euler model [5] to various levels of viscous turbulent flow models [6-12].

The close proximity of adjacent blade rows means that the interactions between relatively moving upstream and downstream blade rows need to be included. The strong 3D nature of the flow field in rotating blade passages points to the first order importance of matching radial flow variations and balance from one blade row to another. Denton instigated the mixing-plane concept to pass the pitchwise mixed out properties across an interface between rotor and stator blade fixed mesh domains, subject to the overall conservation as first reported by Denton & Singh 1979 [13]. This approach allows again a single-passage steady flow solution to be obtained in each blade row while passing the pitchwise averaged radial flow disturbances across the interface, hence satisfying the important requirement of capturing the radial interaction within each blade row and between blade rows. It has to be pointed out that the mixing-plane approach, ever since its inception, has been the main working method in turbomachinery blade aerodynamic designs.

In order to include the blade-row unsteady interaction efficiently without resorting to expensive full unsteady CFD calculations, Adamcyzk 1985 [14] proposed a new framework of the 'average-passage' approach. The approach is developed to capture the influence of periodically passing non-uniform flows of blade passages in an adjacent relatively moving bladerow. In essence, the framework deals with the nonlinear interaction between the mean-flow and the non-uniform (steady/unsteady) disturbances, thus is a manifestation of the general Reynolds-averaging (for turbulence as we know it) in a turbomachinery context. The formulations of Adamczyk are effectively a modelling effort of closing the extra nonlinear product terms due to the averaging, as for turbulence. The framework of the deterministic stresses (DS) is profoundly informative. The impact of the approach will have to depend on how these DS terms are closed. Similar to RANS: low-fidelity models are more efficient but subject to more empiricism.

Higher-fidelity URANSs for blade row interaction, starting to emerge in 1980s, have to face a common challenge: non-equal blade counts for rotor and stator lead to the requirement for a multi-passage (or even whole annulus) computational domain. Take a widely used steady single-passage mixing-plane method as a reference. With the same single-passage domain, making the solution time accurate (e.g. by using the dual time stepping, Jamesson 1991 [15]) will typically consume at least by an order of magnitude more computational time. On top of that, the need for solving a multi-passage/whole annulus domain may add further up to two orders of magnitude of computing cost. Therefore, the conventional direct URANS solutions can be by 3 orders of magnitude more costly, measured against to the standard lower-fidelity but working method.

1.2. Aeroelastic Models: 'Tuned Cascade' for Blade Flutter and Forced Response

The need to predict blade aeroelastic problems (flutter and forced response) for design applications has been a major driver in developing unsteady flow methods. In these cases, the breakdown of the direct blade-to-blade periodicity arises from the basic feature that blade structural dynamic modes typically have a different number of nodes (nodal diameters) than the number of blade passages. Then, unsteady flow due to vibrating blades does not satisfy a simple blade-to-blade periodicity. The travelling wave pattern of the aeroelastic modes follows the well-established 'tuned cascade' model by Lane 1956 [16]. It means that there is a so-called 'phase-shift periodicity'. A phase-shift periodicity is formed on the basis that adjacent blade passages should see the disturbances of the same amplitude but with a constant temporal phase angle difference. Early unsteady aerodynamic methods are mostly of a purely time-linear model based

on a uniform base flow or a time linearized harmonic model based on a nonuniform steady base flow [17-26]. A single-passage linear or linearized unsteady harmonic model can be easily realized numerically with the phase-shift periodic condition.

The development of computer hardware with availability of parallel computing has made it possible that direct nonlinear unsteady solutions of flow in a multistage whole annulus domain can be executed. While direct nonlinear time-domain solutions have made a huge impact on enhancing our understanding of complex flow physics and interaction mechanisms, the computing resources required are also increased significantly in proportion. Compared to a steady flow solution a direct unsteady RANS solution will typically require by 3 orders of magnitudes more computing time, e.g. as discussed by He 2003 [27].

Thus, we note that for the two seemingly different problems: bladerow aerodynamic interaction and blade aeroelasticity, we face more or less the same challenge: a single blade passage model with a direct periodicity is no longer valid while a full-blown multi-passage solution requires a huge step-change increase in computational cost. One can always say that these "today's problems" of high computing cost will become doable 'tomorrow' given ever-increasing computer power. We should be minded to ask, are there any more efficient alternatives, which might help not only solve "today's problems", but also possibly tackle "tomorrow's" in time?

A relevant observation is that all working turbomachinery blades (including those most advanced, most efficient and most highly loaded ones) so far have been designed by using the single-passage steady flow methods. This implies that the steady flow model can be a useful basis, even when unsteadiness makes a non-negligible impact. Given the step-change in the increased computing resources as required by the direct full scale unsteady solutions, there is naturally an incentive to extend the single-passage and steady flow type of methods to unsteady flow computations rather than simply going for the direct multi-passage unsteady solutions in a design environment. We should also keep in mind that 'aerodynamics is only part of the problem'. The future high performance turbomachines for air and land based applications will be increasingly designed in a highly concurrent multi-disciplinary environment. It is against this background that the requirement for developing efficient and accurate methods is called for.

1.3. Brief Overview of Fourier Methods Development

The background overview given above underpins the overall motivation for the development of the Fourier modelling approach. In general, the Fourier spectrum can be used to approximate nonlinear flow disturbances in space and/or in time. In a RANS/URANS framework for the prevalent flow with turbulence filtered (modelled), a Fourier spectrum becomes an efficient and accurate modelling option to pursue for turbomachinery unsteady flows with clearly identifiable periodicities for both blade aeroelasticity and blade-row interaction.

The first effort in using the Fourier series in the nonlinear unsteady turbomachinery flow was made in the development of a time-domain single-passage solver using a Fourier spectral 'shape-correction' by He 1989 [28]. This 'shape-correction' is in conjunction with the phase-shift periodic boundary conditions for situations with disturbances of one fundamental frequency. As a matter of fact, the use of Fourier series for the phase-shift periodicity was initially motivated mainly to overcome the then huge memory consumption needed for low frequency flutter

predictions when using the 'Direct Store' method for the 'phase-lag' periodicity developed by Erdos et al 1977 [29]. Later the Fourier 'shape correction' model was generalized to include multiple disturbances with multiple fundamental frequencies by He 1992 [30]. The time-domain Fourier single-passage phase-shift method was adopted and further developed for multiple blade row configurations by Dewhurst & He 2000 [31], Burgos & Corral (2001) [32], Schnell 2004 [33], Li & He 2002 [34], 2005 [35], Stapelfeldt et al 2015 [36] [37]. The method of using Fourier-series in the blade passage phase-shift periodic boundary condition was further extended by Gerolymos et al 2002 [38].

A more efficient framework than the time-domain use of Fourier spectrum follows the frequency domain approach. The key factor in the computational inefficiency of unsteady flow solutions is the requirement for time-accurate integration. This can be avoided in a frequency-domain harmonic solution of periodic unsteadiness. A framework with an asymptotic expansion for expressing the unsteady harmonic perturbations about a steady base-flow was put forward by Giles 1992 [39]. It is one way influence of a steady base flow on the unsteadiness without feedback influence on the time-averaged flow. A simultaneous two-way coupling approach between the time-averaged flow and the harmonic unsteadiness was proposed by He 1996 [40]. This is effectively a 1st order harmonic balance leading to $2N_f+1$ equations for N_f harmonics. The coupled solution includes the nonlinear interaction between the time-averaged flow and harmonic unsteadiness. The method was thus called 'Nonlinear Harmonic Method', as implemented and demonstrated for unsteadiness of a single fundamental frequency by He & Ning 1998 [41], Ning & He 1998 [42], Chen et al 2001 [43], and for disturbances of multiple-fundamental frequencies by He et al 2002 [44].

A full nonlinear harmonic balance formulation was presented by Hall et al 2000 [45], 2002 [46]. It is worth noting that the authors emphasized the extra cost of including the cross-coupling flux terms among harmonics. The eventual working approach adopted by Hall et al 2002 [46] is essentially a collocation time-spectral method of solving the augmented nonlinear flow equations at $2N_f+1$ time instants in a period. This is a simpler and more efficient procedure than their initial full harmonic-balance one. A similar nonlinear harmonic frequency-domain method was developed by McMullen et al 2001 [47], 2002 [48]. Various further developments, demonstrations and applications have been also made subsequently [49-63].

All these frequency-domain approaches follow the same Fourier modelling principle and share the same basic feature that an unsteady solution retaining N_f harmonics will cost equivalently to $2N_f+1$ steady solutions. Furthermore, these steady-like solutions can be obtained in a multirow domains with only single-passage per bladerow (regardless of blade counts). Thus, URANS simulations of complex component interactions, which would otherwise be hugely costly for conventional multi-passage/whole annulus domains, have become feasible. A notable marker is the URANS simulation of fully coupled compressor, combustor and turbine (Romagnosi et al 2019 [64]) using the nonlinear harmonic method developed, validated and demonstrated by NUMECA (Vilmin et al 2006 [65], 2009 [66]). This is thought to be the first time that such a full-engine unsteady simulation has been conducted with realistic blade counts for the fully coupled core turbomachine components.

In addition to the use of the temporal Fourier model for solutions of nonlinear unsteady flows,

efforts have also been made in developing the spatial Fourier modelling approach. In particular, the spatial Fourier models are developed for circumferential aperiodic and non-axisymmetric duct flows and other applications, either due to deterministic unsteadiness (He 2006 [67], Romero and Corral 2020 [68], Corral et al 2024 [69]) or self-excited flow instabilities of limit-cycle unsteadiness (He 2011 [70], Romero & Corral 2021 [71]).

In the following sections, we will first touch on some general basics and then look at what each of these different Fourier modelling options would entail, from both methodology and application perspectives.

2. Space Time Phase-Shift Periodicity

A key factor in computational efficiency for turbomachinery flow simulations and analyses is the modelling capability to truncate the flow solution domain from a whole annulus of a large number of blade passages (typically 20-100) to a single blade passage. For a steady flow computation truncating all circumferentially non-uniform disturbances from upstream and downstream blade rows, a simple and direct blade-to-blade periodicity can be assumed and easily applied. This direct blade-to-blade periodicity might also be used in a single-passage domain for unsteady flow, but only for an unrealistic case where the circumferential wavelength of the unsteady disturbance is the same as the pitch length of the blade passage (e.g. both rotor and stator rows would have to have the same number of blades). For most practical unsteady flow situations, the direct blade-to-blade periodicity cannot be applied. However, the unsteadiness of interest can be associated with (or decomposed into) one or few disturbances in a circumferential travelling wave form, for which a phase-shift periodicity can be defined. This is indeed the case for the two basic types of unsteady flow problems of interest: rotor-stator bladerow interaction and blade aeromechanics/aeroelasticity. The phase-shift periodicity has been long established in classic time-linear turbomachinery aeroelastic theories and more recent time-linearized numerical analyses. We will take a brief look at the corresponding blade aeroelastic scenario first and how it similarly applies to aerodynamic bladerow interactions as well.

2.1. Phase-Shift Periodicity in Blade Aeroelasticity

For typical turbomachinery aeromechanic problems (i.e. blade flutter and forced response), structural dynamic vibratory patterns of blade and disk assemblies are typically in a cyclic symmetry mode, rotating circumferentially at a constant speed. For this kind of travelling wave modes, the radial lines with zero displacements are called 'nodal diameters'. The circumferential wavelength is defined by the number of nodal diameters. As such the adjacent blade passages in one blade row will have to 'see' the same disturbance pattern but at a constant time-difference (Fig.1). This constant time-difference is predetermined by the relative rotating speed of the structural mode and its circumferential wavelength. Given the number of blades N_b and the number of nodal diameters n, the constant time difference is equivalent to a constant phase lead or lag, called "Inter Blade Phase Angle" σ (in radians):

$$\sigma = \pm\frac{2\pi\, n}{N_b} \qquad (n = 1, 2, .. , N_b/2) \qquad (1)$$

Hence, for a given number of blades of the blade row, σ also defines the circumferential wave-length in terms of the blade pitch length. Typically a flutter instability corresponds to an inter

blade phase angle with a small number of nodal diameters.

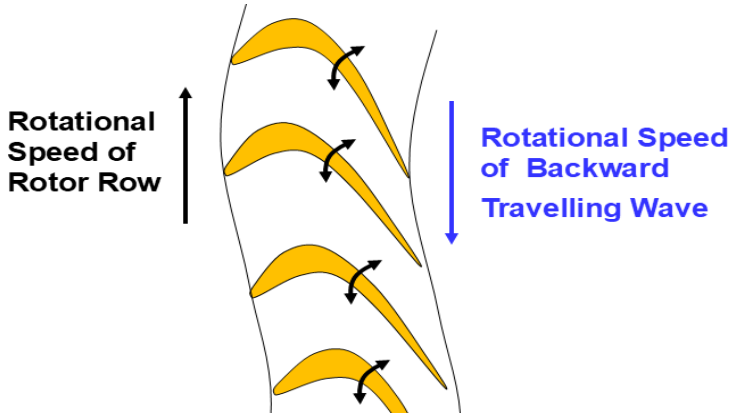

Figure 1: Blade Vibration in Constant Speed Travelling Wave Form ('Tuned Cascade')

2.2. Phase-Shift Periodicity in Rotor-Stator Interaction

For rotor-stator bladerow aerodynamic interactions, the same principle applies. It is perhaps easier to visualize the situation from a purely kinematic point of view. Let's consider the rotor blade row in a compressor rotor-stator stage, as shown in Fig.2. The flow disturbances experienced by each blade at any time instant are completely determined by the relative position of this blade in relation to other blades in both its own row and in the adjacent row. For a rotor passage between Blade A and Blade B. at instant t_1, the trailing edge of the upper blade (B) of the rotor row 'sees' the leading edge of a blade of the stator row (Fig.2a). At t_2, the trailing edge of the lower blade (A) 'sees' the leading edge of another blade of the stator row (Fig.2b). The blades in each blade row are geometrically identical. Regardless of how complex the unsteady flow interactions may be, it then follows that the instantaneous flow field around the upper blade (B) at t_1 must be the same as that around the lower blade (A) at t_2. The time difference between t_1 and t_2 is determined by the blade numbers of the two blade rows and the relative rotational speed between the two blade rows.

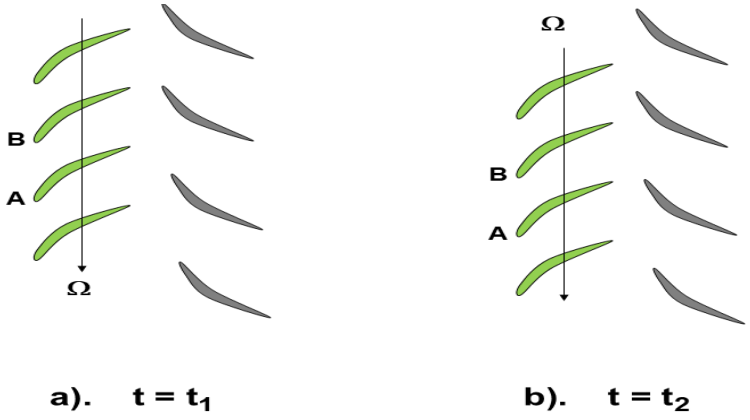

Figure 2: Phase-shift periodicity for rotor blade passage between blade 'A' and blade 'B'

We can similarly work out the corresponding temporal phase angle difference for each row. If a row of N_b blades is subject to unsteady disturbances (wakes and/or non-uniform pressure field) generated by an adjacent blade row with M_b blades, the corresponding inter blade phase angle

(IBPA) would be:

$$\sigma = 2\pi \frac{M_b}{N_b} \tag{2}$$

Here, some comments on the sign of the IBPA should be made. A simple convention is that for the blade passage concerned, if the rotating disturbance is circumferentially travelling in the same direction as that of the rotor rotation, the disturbance is said to be a 'forward travelling wave', and the corresponding IBPA should be positive. On the other hand, if the disturbance is circumferentially travelling in the direction opposite to that of the rotation, the disturbance is said to be a 'backward travelling wave' with a negative IBPA. This convention has been widely adopted in turbomachinery blade aeromechanics, and the same convention can be applied to the blade row interaction. Given that the phase angle between adjacent blades can take positive or negative values, the term 'phase-shift' rather than 'phase-lag' (as often used to refer to the kind of single-passage methods) should be more appropriate.

3. Time-domain Fourier Methods

3.1 Single-passage Fourier Solution *(Single Disturbance)*

The fundamental requirement for use of a Fourier model is the existence of periodicity. The phase-shift periodicity identified in unsteady flows for both blade aeromechanics and bladerow aerodynamic interactions means the Fourier model should be appliable for these problems. As the first attempt in developing a Fourier model for nonlinear unsteady turbomachinery flow computations, the temporal Fourier series is used in truncating a whole annulus to a single blade passage domain. The flow equations in the single-passage domain are still solved by the time-marching, whilst the Fourier series is used at the blade-to-blade periodic boundaries (Fig.3).

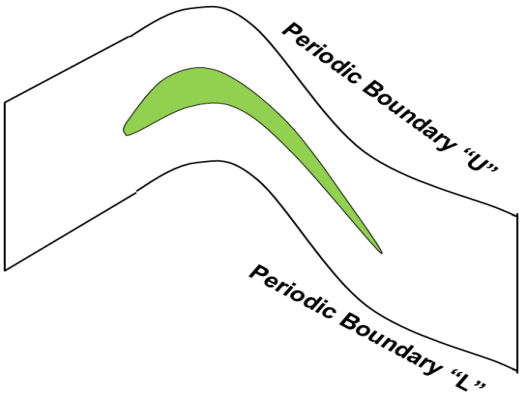

Figure 3: Single-passage domain between two geometrically 'periodic' boundaries

The boundary conditions at the 'periodic' boundaries of a single-passage domain require the link of flow variables between the two boundaries with a constant phase-shift, σ (Inter Blade Phase Angle). The method is called 'Shape-Correction' (He 1989 [28]). The temporal variation (*shape*) of the flow variables is approximated by the Fourier series. During the time marching solution, the execution of the boundary conditions is effectively for the two approximate Fourier 'shapes' at the pair boudnaries to continuously *correct* each other according to the phase-shift periodicity. The correction carries on until a temporal periodic state is reached when the phase-shift periodicity is completely satisfied.

For a single-passage domain (Fig.3), we write a temporal Fourier series retaining N_f harmonics for the flow variables at the lower 'periodic' boundary (U_L) and the upper one (U_U) as:

$$U^L(x,t) = \overline{U}(x)^L + \sum_{n=1}^{N_f}[A_n^L \cos(n\omega t) + B_n^L \sin(n\omega t)] \quad (3a)$$

$$U^U(x,t) = \overline{U}(x)^U + \sum_{n=1}^{N_f}[A_n^U \cos(n\omega t) + B_n^U \sin(n\omega t)] \quad (3b)$$

where $\overline{U}(x)$ is the time-averaged value. Then the Fourier series can be used to correct the current solution at the two boundaries accordingly. For most practical situations of interest, first few harmonics (typically less than 5) are shown to be sufficient. The phase-shift periodicity requires firstly for the time-averaged flow:

$$\overline{U}(x)^U = \overline{U}(x)^L \quad (4a)$$

For a given inter blade phase angle σ, the nth harmonic for the two corresponding mesh points must also satisfy:

$$A_n^U = A_n^L cos(n\sigma) + B_n^L sin(n\sigma) \quad (5a)$$

$$B_n^U = -A_n^L sin(n\sigma) + B_n^L cos(n\sigma) \quad (5b)$$

$$A_n^L = A_n^U cos(n\sigma) - B_n^U sin(n\sigma) \quad (5c)$$

$$B_n^L = A_n^U sin(n\sigma) + B_n^U cos(n\sigma) \quad (5d)$$

The temporal 'shapes' in terms of the Fourier harmonics are updated by a simple discrete Fourier transform (DFT). If N_p is the number of time steps in one period of the fundamental frequency (ω), we then have:

$$A_n = \frac{2}{Np}\sum_1^{N_p} U\, cos(n\omega t) \quad (6a)$$

$$B_n = \frac{2}{Np}\sum_1^{N_p} U\, sin(n\omega t) \quad (6b)$$

Typically, the single passage solution tends to be slow in convergence in comparison with a direct solution. It can be seen from the Fourier summations (Eq.6) that the Fourier harmonic coefficients can only be updated once every period. This delayed updating leads to a slow convergence rate. Generally, it is observed that in comparison with a direct multiple-passage solution, the Shape Correction method tends to require at least twice more time steps to converge to a periodic solution. In other words, the single-passage solution can only provide a saving in computational time if the solution domain of the multiple-passage direct solution counterpart contains more than 3 blade passages.

Here is an example of URANS solutions for NASA Rotor-67 subject to inlet distortion. Fig.4 shows the mesh and some steady flow validation. Fig.5 shows unsteady results under the inlet distortion of single-passage (SP) vs. multi-passage (MP) solutions (Li & He 2002 [34]). We see good agreement between them for both unsteady (Fig.5a) and time-averaged parts (Fig.5b). The latter in comparison with the steady solution also shows clear nonlinear effects well captured by the Fourier method.

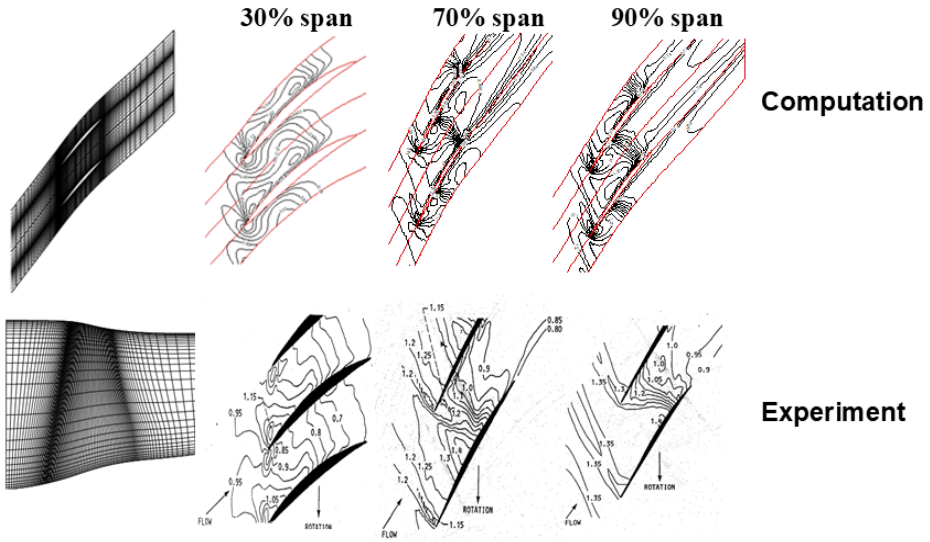

Figure 4: Computational Mesh and Relative Mach Number at 3 Span Sections [34]

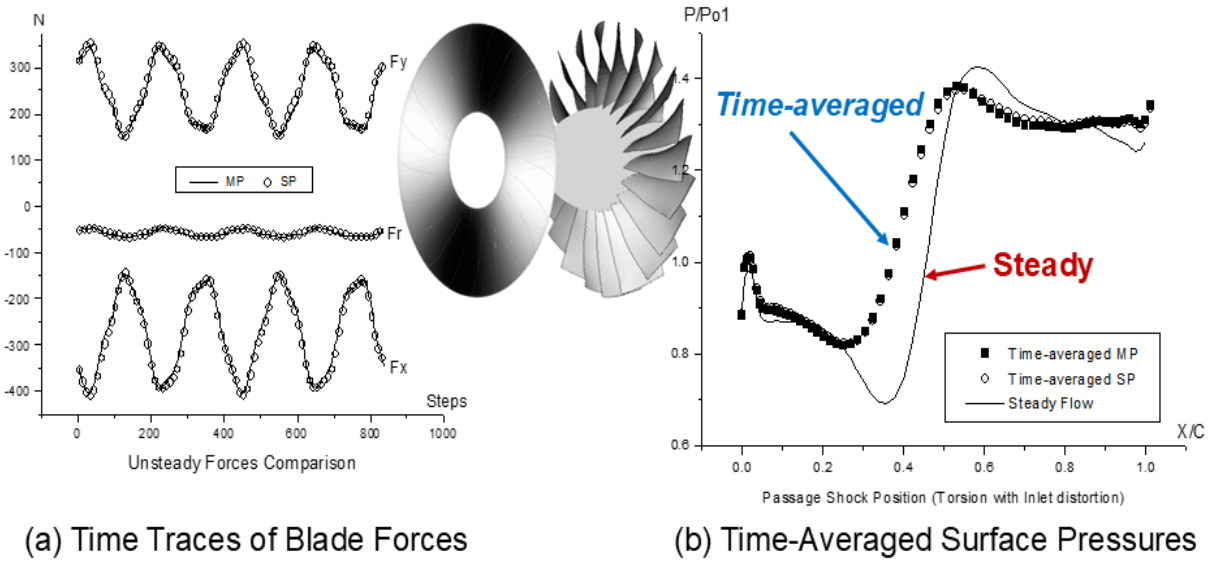

Figure 5: Single-Passage (SP) vs Multi-passage (MP) Solutions [34]

3.2 Single-passage Solution *(Multiple Disturbances)*

A major enabling feature of expressing unsteadiness in a Fourier spectrum is the ability to include multiple disturbances with unrelated frequencies. If we have a total of N_D primary unsteady disturbances with N_D distinctive frequencies respectively, a flow variable at a periodic boundary can be expressed in the following general form, as first introduced by He 1992 [30]:

$$U(x, t) = \overline{U}\ (x) + \sum_{i=1}^{N_D} U_i(x, t) \qquad (7)$$

$\overline{U}(x)$ is the overall time-averaged value. Each unsteady disturbance U_i is identified by its

fundamental frequency ω_i and a corresponding Fourier series containing N_{fi} harmonics:

$$U_i(x, t) = \sum_{n=1}^{N_{fi}} \left[A_{n_i} \cos(n\omega_i t) + B_{n_i} \sin(n\omega_i t)\right], \qquad (i = 1, 2, \ldots N_D) \tag{8}$$

A major issue faced in implementing the generalized Fourier model (Eqs.7, 8) is how to carry out the discrete Fourier transform (DFT) for each disturbance. The numerical integration to work out the Fourier harmonic coefficients needs to be carried out for one period of this disturbance (e.g. Eq. 6). With flow variables containing multiple disturbances with distinctive frequencies, a direct integration will have to be carried out for a time period long enough so that all the disturbances can beat (i.e. this time period will have to contain integer numbers of the periods of all the disturbances concerned). This beating period can be too long to be practical.

A technique to avoid this difficulty is to make use of the existing Fourier harmonics during the integration to work out new harmonics. This is the 'partial substitution' technique as first used by He 1992 [30]. The harmonic coefficients for the i^{th} disturbance are evaluated through the following:

$$A_{ni} = \frac{2}{Np_i} \sum_1^{N_{pi}} (U - R_i) \cos(n\omega_i t) \tag{9a}$$

$$B_{ni} = \frac{2}{Np_i} \sum_1^{N_{pi}} (U - R_i) \sin(n\omega_i t) \tag{9b}$$

where $R_i = \sum_{j \neq i}^{N_D} \sum_{n=1}^{N_{fj}} \left[A_{nj} \cos(n\omega_j t) + B_{nj} \sin(n\omega_j t)\right]$ is the contributions from all disturbances except that from the i^{th} disturbance. Now, for the i^{th} unsteady disturbance, new values of the Fourier coefficients can be obtained after one period of the disturbance (N_{pi} time steps), when the partial-substitution (Eq.9) is used.

A partial substitution technique has also been adopted by Gerolymos et al 2002 [38], which leads to an effective formulation for a continuous updating of the Fourier harmonics with time steps. For a single disturbance, the harmonic coefficients for a new time step *m* can be updated by a correction on those at the previous step *m-1*. For the *nth* harmonic coefficient, we then have,

$$(A_n)_m = (A_n)_{m\text{-}1} + \frac{2}{N_p} \cos(n\omega t_m)(U_m - U_{m-Np}) \tag{10a}$$

$$(B_n)_m = (B_n)_{m\text{-}1} + \frac{2}{N_p} \sin(n\omega t_m)(U_m - U_{m-Np}) \tag{10b}$$

where U_{m-Np} is the flow variable at the time one period earlier and can simply be approximated by using the existing Fourier series at m-1.

Here we see a multi-disturbance example of a transonic rotor embedded between two stator rows: a frontal row of inlet guide vanes (IGV) and a downstream stator (Li & He 2005 [35]). The blade counts are: N_{IGV}=33, N_{Rotor}=57, and N_{Stator}=58. The single-passage method is validated against the multi-passage solution (Fig.7), and then used to predict aerodynamic efficiency and aeroelastic stability (aero-damping) at different intra-blade row gaps, shown in Fig.8.

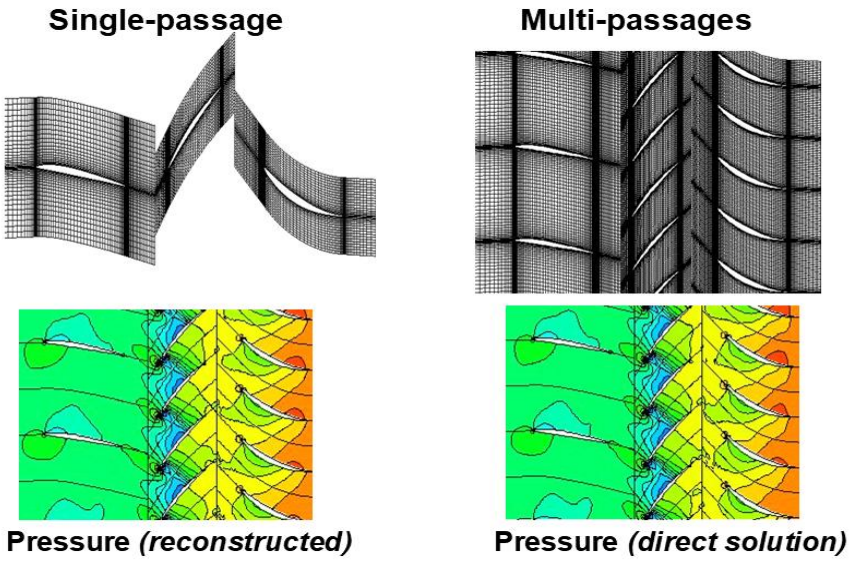

Figure 6: Computational Mesh and Unsteady Pressures (Single-passage vs. Multi-passage) [35].

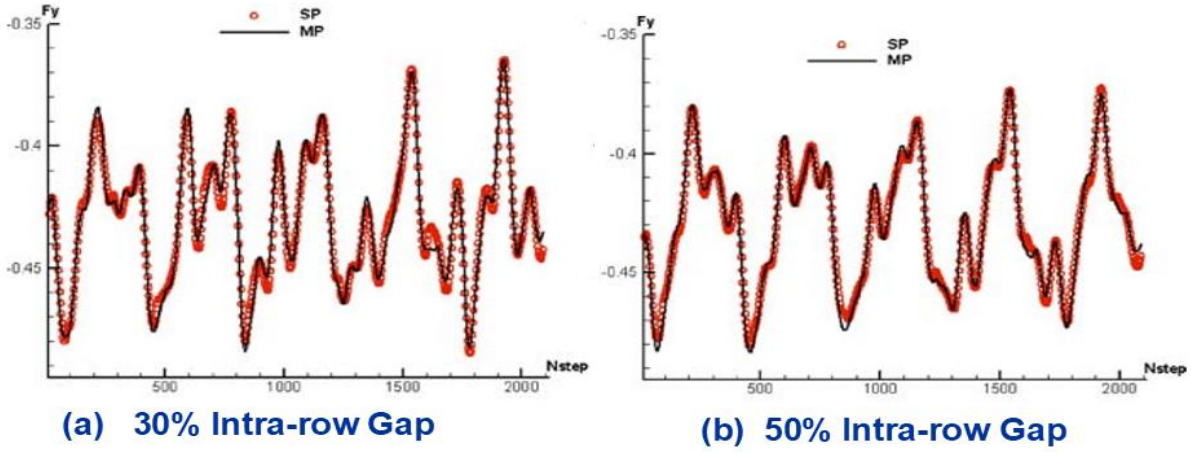

Figure 7: Unsteady Blade Forces in Time, Single-passage (SP) vs. Multi-passage (MP) [35].

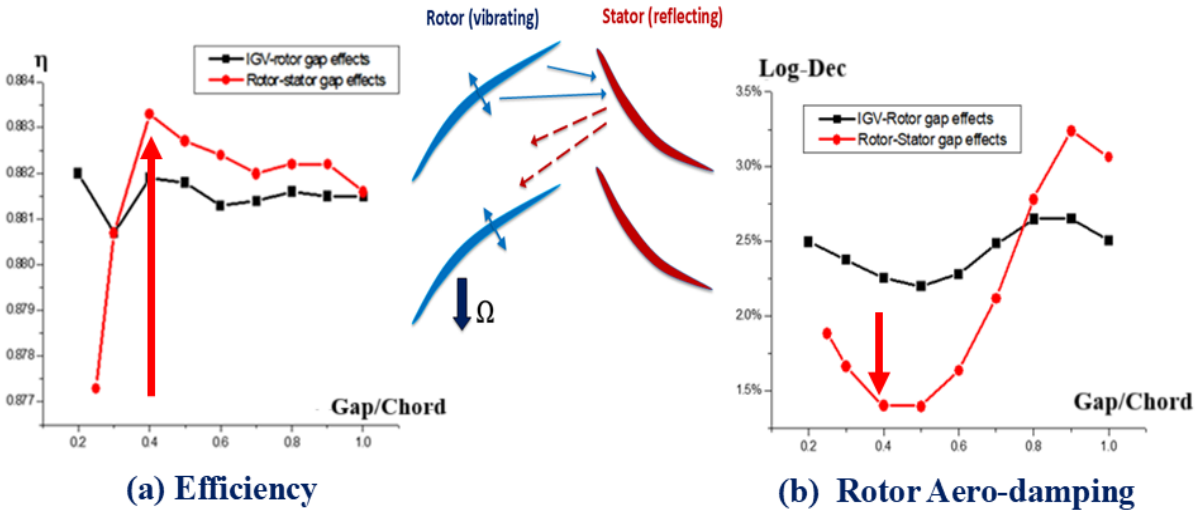

Figure 8: Intra-row Gapping Effects (Aero-efficiency vs. Aero-damping) [35].

The performance sensitivity is largely dictated by the roro-stator gap (the lines in red). Special attention is paid to a 40% rotor-stator gap (highlighted in Fig.8). This is where we see a maximum efficiency (Fig,8a), but also a minimum aero-damping (Fig.8b). This conflicting characteristics observed highlight the importance of multi-disciplinary interactions in a design process.

3.3. Spatial Fourier Solutions based on Discrete Mesh Blocks ('Block-Spectral' Model)

The methods described above are all for timewise periodic unsteadiness. The Fourier modeling can also be used in space to reduce computational resources. A particular effort here is to extend the method to situations with non-axisymmetric steady and unsteady flows, e.g. those encountered in an intake duct or a rotor/stator disc cavity.

Consider a circumferential non-uniform flow with a wavelength of the whole annulus. Taking a cylindrical coordinate system (x, r, θ), we approximate the instantaneous circumferential variation by the Fourier series with N_f spatial harmonics:

$$U(x, r, \theta, t) = \bar{U}(x, r, t) + \sum_{n=1}^{N_f} [A_n(x, r, t)\cos(n\theta) + B_n(x, r, t)\sin(n\theta)] \quad (11)$$

where $\bar{U}$ is the circumferentially averaged value. The Fourier coefficients A_n and B_n also only depend on the axial and radial coordinates. Similar to the temporal Fourier series, we have $2N_f+1$ unknowns. Note, however, $\bar{U}$, A_n and B_n are now all time-dependent. Hence we need to determine the $2N_f+1$ unknowns to fix the Fourier series simultaneously at each time step during an unsteady time-marching solution.

The purpose of using the Fourier approximation is to reduce the computing resource required by a direct calculation of the whole 360° circumference. The circumferential domain can be truncated to such an extent as long as it can provide sufficient information to fix the Fourier series. Similar to the Fourier model in time, the minimum requirement for N_f order Fourier series would be $2N_f+1$ points. Now we take uniformly spaced $2N_f+1$ points over the circumference (thus three circumferential mesh cells needed if only one harmonic is retained). In general, $2N_f+1$ mesh cells will be placed in the following circumferential positions for an N_f harmonics Fourier series:

$$\theta_i = \frac{i}{2N_f+1} 2\pi, \qquad (i = 1, 2, \ldots, 2N_f+1) \quad (12)$$

For given flow variables U_i at $2N_f+1$ mesh points, the spatial Fourier shape can be easily obtained by simple summations,

$$\bar{U}(x, r, t) = \frac{1}{2N_f+1} \sum_{i=1}^{2N_f+1} U_i \quad (13a)$$

$$A_n(x, r, t) = \frac{2}{2N_f+1} \sum_{i=1}^{2N_f+1} U_i \cos(n\theta_i) \quad (13b)$$

$$B_n(x, r, t) = \frac{2}{2N_f+1} \sum_{i=1}^{2N_f+1} U_i \sin(n\theta_i) \quad (13c)$$

Once the circumferential Fourier series is determined, the flow variables at any circumferential positions are easily evaluated. For each step, we first use the updated flow variables at the cell centers of $2N_f+1$ cells to carry out the Fourier Transform and then the Fourier series to work out the values at the dummy points, ready for the flux/difference evaluations for the next iteration.

Here are some computational examples for the spatial Fourier model. The first case is for a simple 3-dimensional annulus intake duct subject to a 10° crosswind (He 2006 [67]). The computational mesh for the direct full-domain calculation has 300 circumferential mesh cells covering the 360° annulus domain. At the inlet, circumferential distortions in the circumferential and radial inflow angles are specified. Both the circumferential and radial angle distortions are in a sinusoidal form with an amplitude of 10°. But the two angles are offset by a 90° circumferential phase difference. The Fourier solution (Fig.9a) retaining 5 harmonics needs only 11 circumferential mesh cells for 360° annulus domain. The direct calculation (300 circumferential mesh cells) is shown in Fig.9b.

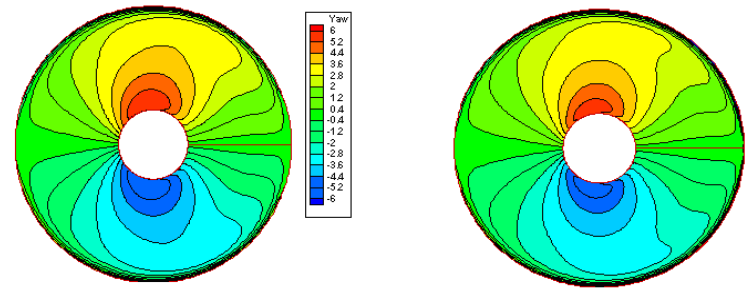

Figure 9: Circumferential Fourier Solution (yaw angle) for intake duct subject to 10° cross-wind [67]

The next example is for an intake duct subject to upstream tone noise propagation from a fan rotor (He 2013 [72]). The rotating pressure disturbances from the rotor of 12 blades are approximated by a specified circumferential traveling pressure wave of 12 nodes (Fig.10a). Given the periodicity, the calculations are carried out in a 1/12th (30°) sector. We will look at the influence of acoustic liner with 500 micro-cavities for one 30° sector (Figh.10b). It is of particular interest to compare a direct solution of resolving all 500 micro-cavities and a Fourier block-spectral solution resolving only a small number of micro-cavities.

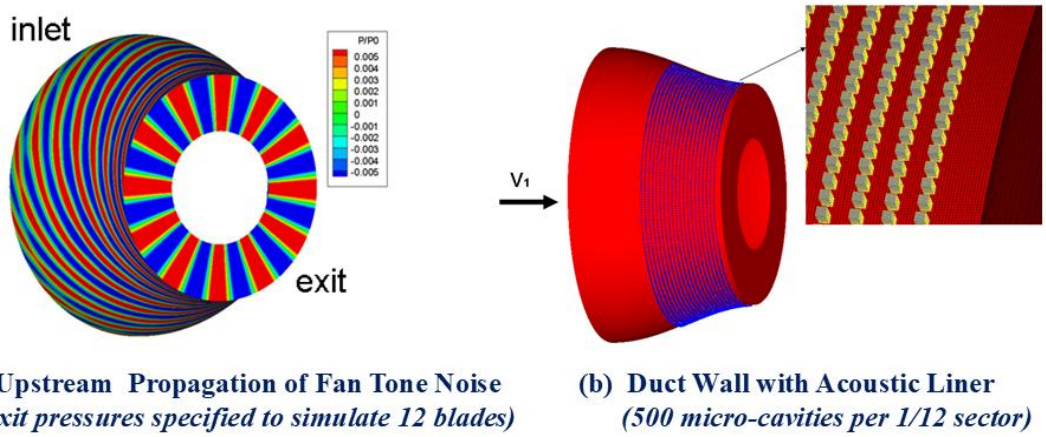

Figure 10: Upstream propagation of fan tone noise generated at intake duct exit [72]

Fig.11 shows the predicted instantaneous pressure/noise disturbances. In this case, the near-casing part is acoustically cut-on, while the bulk of the inner region of smaller radii is cut-off. Thus, the fan blade tone noise can propagate upstream near casing, most strongly for the smooth wall case (Fig,.11a). The noise reduction effect due to the liner is also clearly seen (Fig.11b).

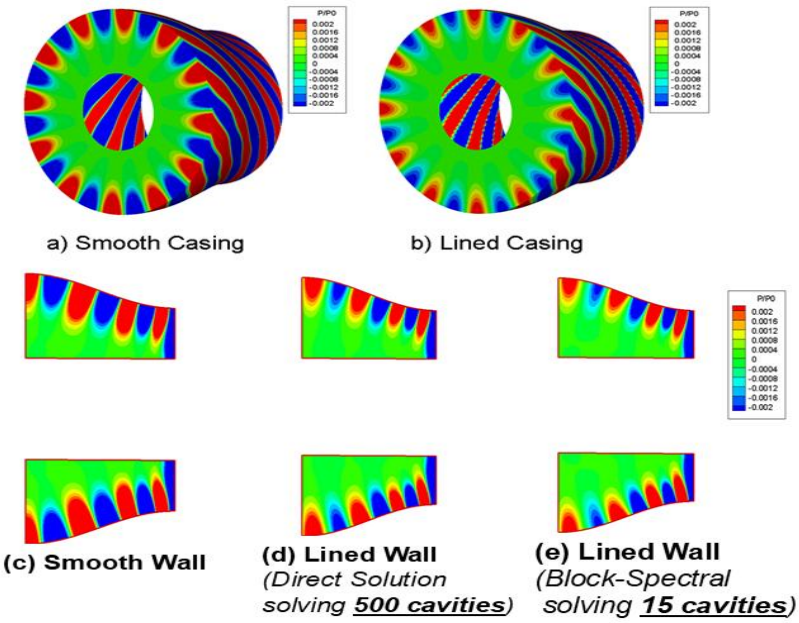

Figure 11: Upstream propagation of fan tone noise and influence of casing wall liner [72]

The unsteady pressures on the meridional plane (Figs.11c, d, e) clearly show that the impact of the liner can be well predicted by using the Fourier block-spectral method, which solves only 15 micro-cavities (Fig.11e) in contrast to the direct solution of solving 500 cavities (Fig.11d).

Another example is a self-excited unsteady flow. Consider a rotor-stator disc cavity. At certain conditions, non-axisymmetric self-sustained unsteady flow patterns may occur in a cavity of axisymmetric geometry and flow conditions (Owen [73], Bohn et al [74]). Given the self-excited characteristics with unknown frequencies, a time-domain approach is needed. The results shown in Fig.12 (He [70]) are for the rotating cavity configuration of Bohn et al [74].

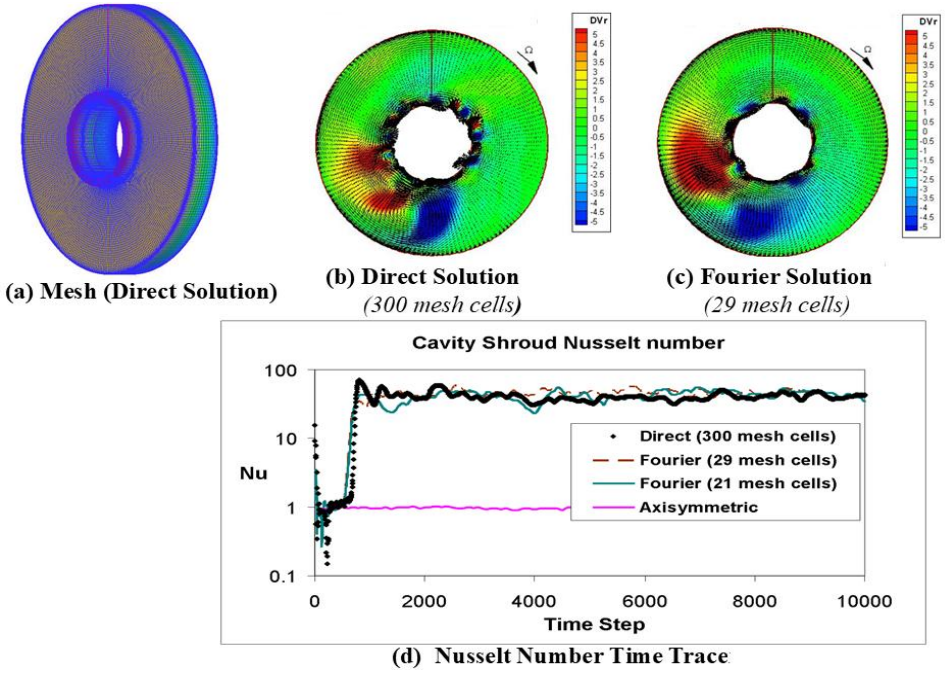

Figure 12: Buoyancy-driven unsteady flow and heat transfer in rotating cavity [70]

The instantaneous radial velocity disturbances indicate one pair vortex pattern predicted by a direct solution (Fig12b) compared to the Fourier solution (Fig.12c). Fig.12d shows the time histories of Nusselt number on the rotating cavity outer boundary. Two Fourier solutions with 10 harmonics (21 mesh cells) and 14 harmonics (29 mesh cells) respectively compare well with the direct solution (300 mesh cells), but they all are qualitatively different from an axisymmetric solution.

4. Frequency-Domain Fourier Methods

The time-domain Fourier approach provides an effective way to solve flow field in a truncated domain with single blade passage (or only few passages), hence a significant speed up, compared to a direct multi-passage solution. However, the solution efficiency is still significantly limited by the time-accurate integration. This is also compounded by the slow convergence caused by the non-simultaneous updating of the Fourier series. Development of frequency-domain methods serves well in addressing this issue. A fundamental feature of frequency-domain approaches is that the problem of time-marching unsteady flow equations is effectively converted to that of solving steady-like flow equations.

4.1. Nonlinear Harmonic Method

4.1.1. Balancing Time-averaged and Unsteady Flow Disturbances Equations

The principal approach can be more simply illustrated by considering the 1-D momentum equation for a compressible inviscid flow with density ρ, velocity u and static pressure P.

$$\frac{\partial \rho u}{\partial t} + \frac{\partial \rho u u}{\partial x} = -\frac{\partial P}{\partial x} \tag{14}$$

Note that the equation is part of the coupled system in the conservative flow variables. Thus the basic decomposition begins with the conservative variables. Take the flow decomposition before introducing the Fourier approximation. The unsteady conservative variables are decomposed into a time-mean and a fluctuation part.

$$\rho = \overline{\rho} + \rho' \tag{15a}$$

$$\rho u = \overline{\rho u} + (\rho u)' \tag{15b}$$

The secondary flow variables are also similarly decomposed in time.

$$u = \overline{u} + u' \tag{16a}$$

$$P = \overline{P} + P' \tag{16b}$$

Thus, with $\frac{\partial}{\partial t}(\overline{\rho u}) = 0$, the expanded full equation is written as (with no assumption made yet):

$$[\frac{\partial}{\partial x}(\overline{\rho u}.\overline{u} + (\rho u)'u') + \frac{\partial \bar{P}}{\partial x}] + [\frac{\partial (\rho u)'}{\partial t} + \frac{\partial}{\partial x}(\overline{\rho u}\, u' + \overline{u}\,(\rho u)') + \frac{\partial P'}{\partial x}] = 0 \tag{17}$$

The terms above are purposely grouped into two, depending on their relevance to the time-averaged flow. The first is for those which contribute directly to the time-averaged flow, whilst the second is for those which don't. The time-averaged equation can be directly obtained by time-averaging the full unsteady time-domain equation. Note that for a given time-averaged flow, all the terms in the second group of Eq.17 are linearly proportional to the corresponding unsteadiness with zero time-mean. The time-averaged equation will thus only contain those of the first group:

$$\frac{\partial}{\partial x}\left(\overline{\rho u}.\overline{u}+\overline{(\rho u)'u'}\right)+\frac{\partial \bar{P}}{\partial x}=0 \qquad (18a)$$

The above equation can also be reached when we balance those unsteady terms in the second group:

$$\frac{\partial(\rho u)'}{\partial t}+\frac{\partial}{\partial x}\left(\overline{\rho u}\,u'+\overline{u}\,(\rho u)'\right)+\frac{\partial P'}{\partial x}=0 \qquad (18b)$$

The following observations should be made.

i) The equations for the time-averaged flow (Eq.18a) and the unsteady flow disturbances (Eq.18b) are inter-dependent, reflecting how the two parts should interact physically.

ii) The importance of the time-averaged flow equation should be underlined. Particularly a time-averaged flow state serves as the base condition on which multidisciplinary multi-component designs (optimizations) are carried out and ranked. For the modelling consistency in reaching the time-averaged flow equation (Eq.18a), all terms in the unsteady fluctuation equation (Eq.18b) need to be in a temporally linear form with zero time-mean.

iii) Given the above modelling consistency requirement, the direct time-averaging based decomposition for primary conservative variables (Eqs.15a, 15b) and secondary variables (Eqs.16b, 16b), should be more appropriate than some other averaging techniques. For example, in Favre-averaging ($u=\tilde{u}+u''$, $\tilde{u}=\overline{\rho u}/\overline{\rho}$), the velocity disturbance u'' has a nonzero time-mean ($\overline{u''}\neq 0$). Consequentially, the corresponding disturbance term in the unsteady equation (Eq.18b) will no longer be temporally linear. Without the modelling consistency, the time-averaged flow equation (Eq.18a) then becomes unwarranted. In a general RANS context, this inconsistency may not be a real issue as the time-averaged equations are to be closed by an empirically established (tuned) turbulence model. However, in the nonlinear harmonic framework in which the time-averaged equation is closed by directly computed harmonic unsteadiness (thus the 'unsteady stresses'), any modelling inconsistency between the time-averaged and the harmonic equations should be avoided.

4.1.2. Nonlinear Harmonic Formulations by Harmonic Balance

We express an unsteady flow variable in a Fourier series with N_f harmonics. For ρu we have

$$\rho u=\overline{\rho u}+\sum_{n=1}^{N_f}\left[\left(A_{\rho u}\right)_n\cos(n\omega t)+\left(B_{\rho u}\right)_n\sin(n\omega t)\right] \qquad (19)$$

We then use harmonic balance for the time-domain unsteady disturbances (Eq.18b). The harmonic equations can be simply obtained by balancing all sine and cosine terms respectively. Including the time-averaged equation (the 0th harmonic), we now have $2N_f+1$ time-invariant equations:

$$\frac{\partial}{\partial x}\left(\overline{\rho u}.\overline{u}+\overline{(\rho u)'u'}\right)+\frac{\partial \bar{P}}{\partial x}=0 \qquad (n=0) \qquad (20a)$$

$$-n\omega\left(A_{\rho u}\right)_n+\frac{\partial}{\partial x}\left[\overline{\rho u}(B_u)_n+\overline{u}\left(B_{\rho u}\right)_n+(B_p)_n\right]=0, \qquad (n=1,2,..,N_f) \qquad (20b)$$

$$n\omega\left(B_{\rho u}\right)_n+\frac{\partial}{\partial x}\left[\overline{\rho u}\left(A_u\right)_n+\overline{u}\left(A_{\rho u}\right)_n+(A_p)_n\right]=0, \qquad (n=1,2,..,N_f) \qquad (20c)$$

Thus, for a single disturbance with a fundamental frequency ω, approximated by N_f harmonics, a time-domain unsteady solution is now equivalent to $2N_f+1$ steady-like solutions (Eq.20). For a general multiple primary disturbance case with N_D fundamental frequencies (Eq.7), He 1992 [30], the number of steady-like solutions similarly scales with N_D as: $2(\sum_{i=1}^{N_D}N_{f_i})+1$.

The time-averaged flow equation (Eq.20a) is simply a zeroth harmonic balance. Its solution depends on the nonlinear stress terms ("Deterministic stresses', Adamczyk [14]), which can now be directly worked out once the harmonics are known. The unsteady stress for two variables X and Y can be simply obtained (e.g. He et al 2002 [44]):

$$\overline{(X)'Y'} = \frac{1}{2}\sum_{i=1}^{N_D}\sum_{n=1}^{N_{fi}}[(A_{Xi})_n(A_{Yi})_n + (B_{Xi})_n(B_{Yi})_n] \quad (21)$$

The unsteady harmonic solutions in turn depend on the time-averaged flow. Thus, all these harmonically balanced equations are closely coupled and solved accordingly [40], [41], [42]. The strongly coupled procedure with iteration steps is depicted in the flow chart (Fig.13). The deterministic stress terms in the time-averaged flow equations are concurrently updated (Eq.21) at each step during the solution process. It is also worth noting that the unknown coefficients of the Fourier spectrum are directly obtained from the solutions to the harmonic balance equations (e.g. $2N_f+1$ equations in Eq.20 for a single disturbance case). As such, Fourier transform is not needed during the nonlinear harmonic solution process.

The nonlinear harmonic model includes the interaction between the time-averaged flow and the harmonics but neglects the higher order cross-coupling between the harmonics. For instance, the product between harmonic terms with frequencies 2ω, and 1ω would generate a contribution to the harmonic at frequency ω, as similarly the harmonics at 3ω and 1ω would do to the harmonic at 2ω. These cross-coupling terms are included in the full harmonic balance formulation presented by Hall et al 2002 [45]. It has been shown that these harmonic cross–coupling terms can also be included in the original nonlinear harmonic method as illustrated by Vasanthakumar 2003 [75].

It should be noted that for a blade aeroelastic analysis, the stability (aerodynamic-damping) needs typically to be evaluated at the frequency of the blade structural dynamic mode (e.g. 1st bending/flap, 1st torsion). It can be shown that the aero-damping (work done on a vibrating blade) will only depend on the harmonic flow force component at the vibrating frequency due to the orthogonality of harmonic modes. If only one harmonic is retained in the Fourier series, the cross-coupling terms between different non-zero harmonics disappear. The nonlinear harmonic model is then equivalent to a fully nonlinear harmonic-balance formulation.

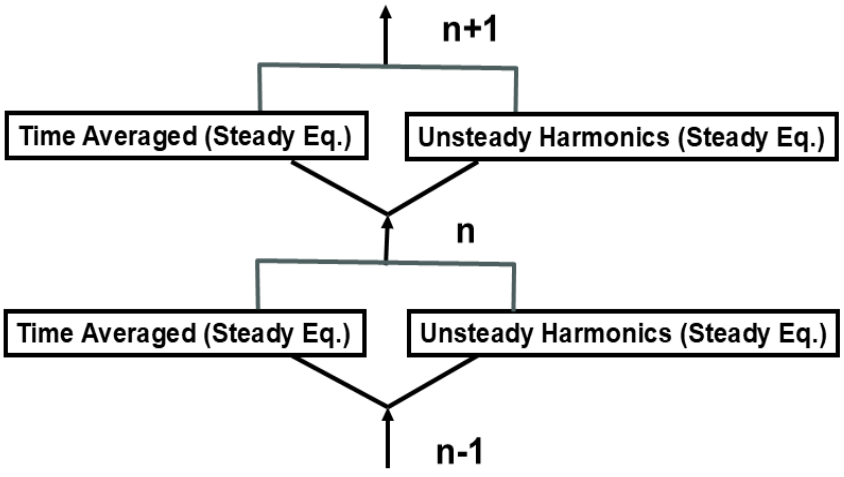

Figure 13: Concurrent Coupling between Time-average Flow and Harmonic Disturbances

4.2. Harmonic Time-spectral Method

A key feature of the work by Hall et al 2002 [46] is the collocation time-spectral procedure used to solve the nonlinear flow equations. Consider the Reynolds-averaged unsteady Navier-Stokes equations (including the equation(s) for a turbulence transport model):

$$\frac{\partial U}{\partial t} = R(U) \tag{22}$$

When retaining N_f Fourier harmonics, we can take $2N_f+1$ time instants t_j, (j =1, 2 … $2N_f+1$) with a constant interval in one period. The flow equations must hold at these time instants respectively:

$$(\frac{\partial U}{\partial t})_j = R(U_j) \qquad (j = 1, 2, \ldots, 2N_f+1) \tag{23}$$

Using the Fourier harmonics to express the time-derivative term ($\frac{\partial U}{\partial t}$), we then have:

$$\sum_{n=1}^{Nf}[n\omega(-A_n\, sin(\, n\omega t_j) + B_n\, cos(\, n\omega t_j)] = R(U_j), \qquad (j = 1, 2, \ldots, 2N_f+1) \tag{24}$$

This set of equations can be simply solved at the $2N_f+1$ time instants respectively. After each solution iteration when the flow variables are updated at these time-instants, all harmonics can be obtained by a discrete Fourier Transform of the $2N_f+1$ solutions. Then the LHS terms in Eq.24 are also updated, ready for the next iteration.

Therefore we see that the harmonic balance is not needed in establishing the $2N_f+1$ time-domain equations, though the method may be labelled as 'Harmonic Balance'. This is in contrast with the nonlinear harmonic method where Harmonic Balance is actually used to set up the $2N_f+1$ harmonic equations (Eq.20), but Fourier Transform is not needed. It is recognized that whether or not the FT is used during a solution process can be consequential in terms of aliasing associated accuracy and stability, especially in cases with multiple disturbances, as further discussed later.

The time-spectral method is simple to implement with relatively small changes to any existing RANS codes. Another appealing feature of this time-spectral implementation is the treatment of turbulence modelling in a frequency-domain model. The inclusion of a turbulence model in a frequency-domain model tends to be non-trivial (e.g. Holmes et al 1997 [76]). In the baseline nonlinear harmonic method, the turbulence model is frozen at the base state to avoid the tedious linearization of the nonlinear turbulence eddy viscosity model around the time-averaged flow [41-44]. With the time-spectral approach, the turbulence transport equations can be easily solved in the same manner as that for other fluid transport equations.

For situations where only one harmonic is retained ($N_f = 1$), a simpler 'phase-solution' formulation can be obtained by taking 3 distinctive phases, $\omega t_1 = 0°$, $\omega t_2 = 90°$ and $\omega t_3 = -90°$ respectively, as demonstrated for a URANS by He 2008 [77]. Then we can directly get the time-averaged and harmonic flow variables, also without needing a Fourier transform:

$$\overline{U} = \frac{U_2+U_3}{2}, \tag{25a}$$

$$A = \frac{2U_1-U_2-U_3}{2}, \tag{25b}$$

$$B = \frac{U_2-U_3}{2}. \tag{25c}$$

The simple harmonic 'phase-solution' method also serves as the basis for the development of a distinctive adjoint based concurrent aerodynamic-aeroelastic design optimization (Wang & He 2009 [78], He & Wang 2011 [79]).

4.3. Harmonic Solution for Multiple Disturbances *(Rotor-Rotor/Sator-Stator Interactions)*

As stated in the introduction to the Fourier method development, one of the main target applications is unsteady multi-stage flow analysis. The accuracy and effectiveness of the 'average-passage' framework (Adamcyzk 1985 [14]) has to depend on how the averaging-led 'deterministic stresses' are closed (just like how Reynolds stresses are closed by turbulence models). The nonlinear harmonic model provides a pathway towards closing the 'deterministic stresses' by directly computing (rather than modelling) them efficiently with the set of steady-like harmonic solutions.

For multi-stage turbomachines, we need to deal with not only interactions between relatively moving rotor and stator rows, but also those between relatively stationary blade rows (rotor-rotor or stator-stator). Typical examples are the time-averaged flow distributions exhibiting the 'Clocking' dependence and 'Aperiodic' passage-passage variations.

Consider a two-stage compressor consisting of rotor-1, stator-1, rotor-2 and stator-2. N_{R1} and N_{R2} denote the blade numbers for rotor-1 and rotor-2 respectively. It is well known that the rotor-rotor interaction is dependent on the blade counts, e.g. as discussed by He et al 2002 [44]. In the case of the rotor-1 and rotor-2 interference, the influence of rotor-1 wake disturbances on rotor-2 needs to be included. The key part to focus on is the inlet to rotor-2 domain (i.e. the interface between stator-1 and rotor-2). Rotor-2 inlet is subject to two distinctively different primary disturbances, a) unsteady interaction between stator-1 and rotor-2; and b) steady-like influence from rotor-1.

Start with the general multi-disturbance model (Eq.7) as proposed by He 1992 [30]. In this case for rotor-2, we have two primary disturbances of two fundamental frequencies (i.e. N_D=2):

$$U(x, t) = \overline{U}(x) + \sum_{i=1}^{2} U_i(x, t) \tag{26a}$$

In the nonlinear harmonic method, the total number of harmonic balanced equations to be solved (including the time-averaged flow as the zeroth harmonic) is $2(N_{f1}+ N_{f2})+1$, where N_{f1} is the number of harmonics retained for the first primary disturbance; N_{f2} for the second primary disturbance. More specifically for rotor-2, we have:

$$U(x, t)_{R2} = \overline{U}(x)_{R2} + U_{S1\text{-}R2}(x, t) + U_{R1\text{-}R2}(x, t) \tag{26b}$$

Given the passage-passage variation in rotor-2, $\overline{U}(x)_{R2}$ for a given mesh point is taken as a passage-average of time-averaged variables at corresponding mesh points of all rotor-2 passages.

To identify rotor-1 wake disturbances, we consider how they manifest in the adjacent downstream stator. In stator-1 domain, rotor-1 wakes are seen as unsteady disturbances in the form of a circumferential travelling wave with a phase-shift periodicity. Thus, at stator-1 exit, any unsteady disturbance in the travelling wave form with the phase-shift periodicity should be seen as 'steady' in the rotor frames. It then follows that the unsteady disturbances at stator-1 exit should correspond to rotor-1 wake disturbances. Rotor-1 disturbances can thus be specified at rotor-2 inlet in a traveling wave form with the corresponding inter-blade phase angle. A key difference in the treatment between the rotor-rotor and the stator-rotor interactions is that a zero frequency is taken for the rotor-rotor disturbances. As such, different clocking and aperiodic time-averaged flow patterns can be simply reconstructed in post-processing from the single-passage nonlinear harmonic solution for any given relative phase angle/clocking between rotor-1 and rotor-2.

An example for a transonic compressor is presented in Figs.14-17 (He et al 2002 [44]).

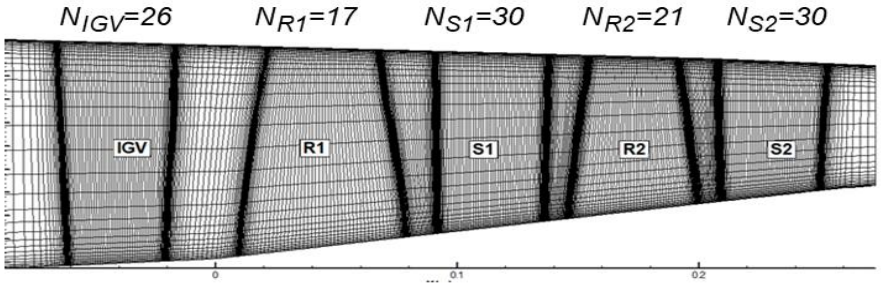

Figure 14: Computational Mesh on Meridional Plane (2&1/2 stage transonic compressor)

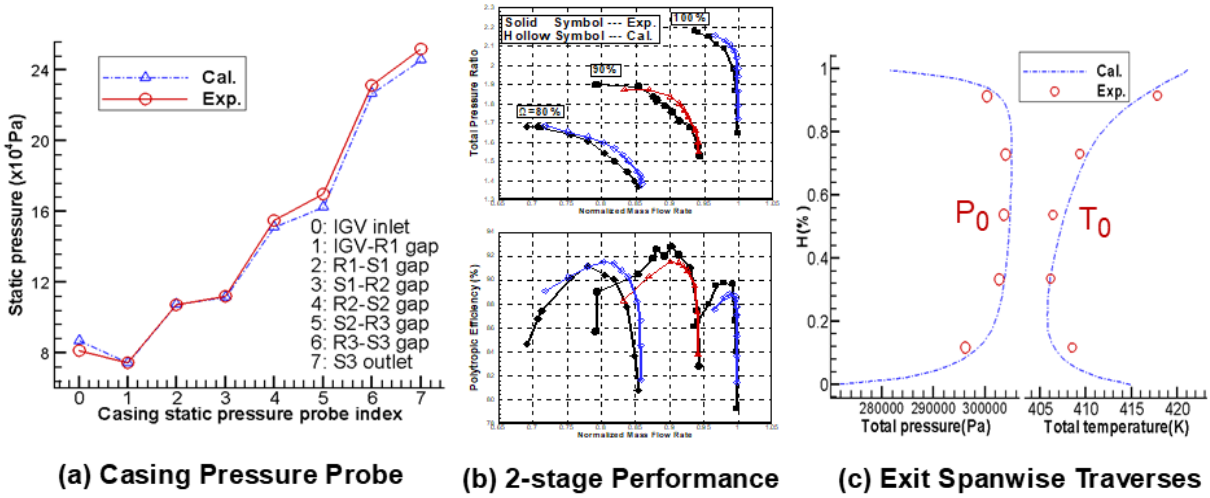

Figure 15: Comparisons with Experimental Data (He et al [44], Wang et al [80]).

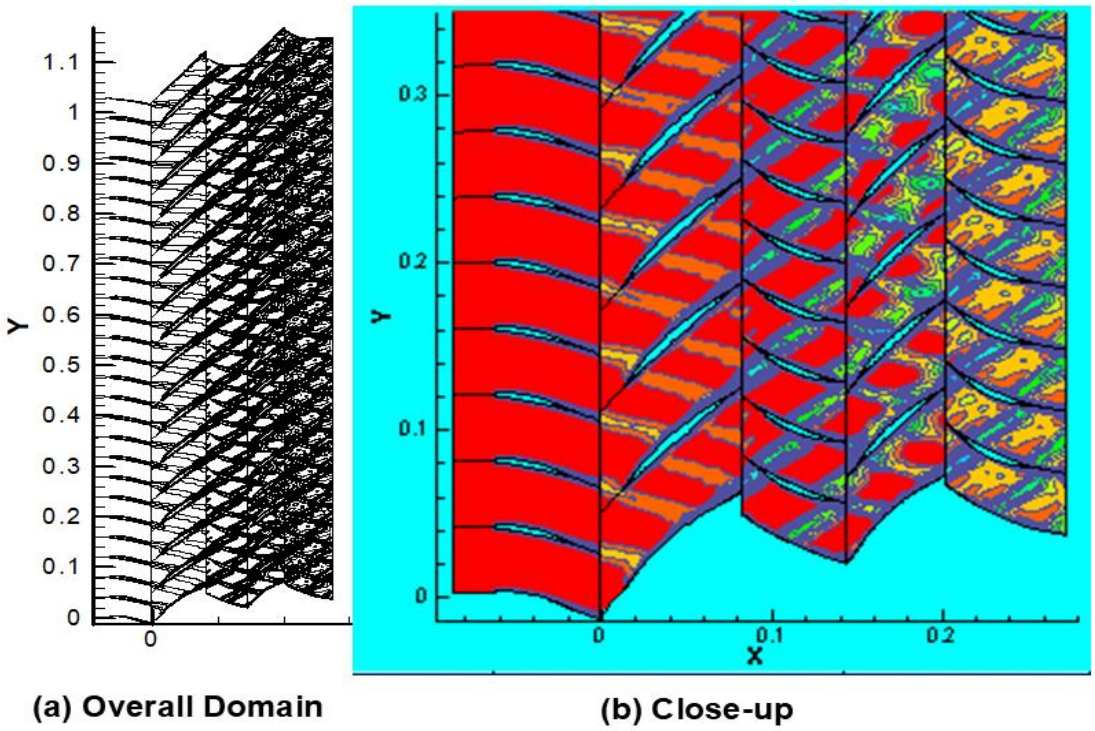

Figure 16: Instantaneous Entropy (constructed from single-passage solution [44]

The stator-stator and rotor-rotor interactions are indicated in the efficiency variations with the relative circumferential position/clocking. Both stator-1 and stator-2 have 30 blades each, leading to a maximum observable stator-stator clocking effect. The clocking effect on the overall efficiency predicted for this case is very small, much lower than 0.1% (Fig.17a). The aperiodic passage-passage variation in Rotor-2 (Fig.17b) shows 4 peaks/troughs as expected from the difference the in blade count between the two rotors (17 and 21). The efficiency variation at rotor-2 exit exhibits a peak-trough difference of about 0.6, which is quite considerable for compressor performance. It seems that rotor-rotor interactions have much more pronounced effects than stator-stator interactions for a transonic compressor, though the stator-stator clocking has been far more studied.

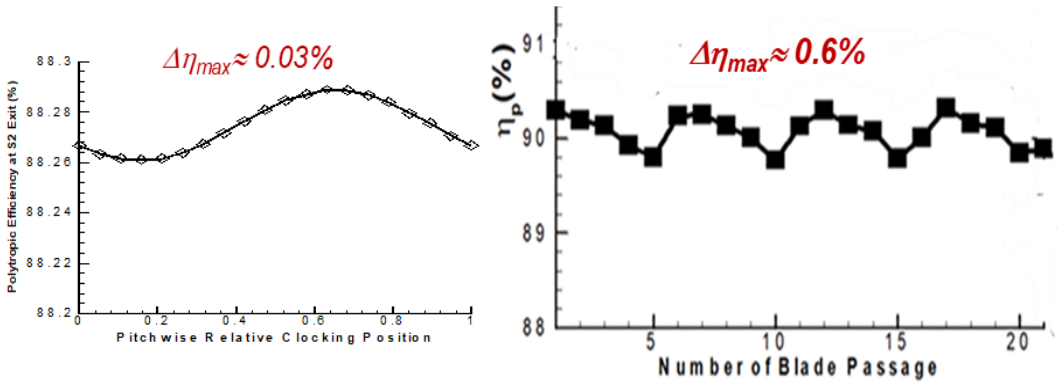

(a) Stator1 - Stator2 Clocking ($N_{S1}=N_{S2}=30$)

(b) Rotor2 Passage Aperiodicity ($N_{R1}=17$, $N_{R2}=21$)

Figure 17: Stator-Stator, Rotor-Rotor Interaction in terms of Efficiency [44]

Before closing the main sections of this lecture, a few further observations are added here.

In terms of computational costs, a single-passage nonlinear harmonic multistage solution with 2-3 harmonics for each primary disturbance is about 8 times of computational time per step compared to a steady mixing-length solution. Given that a harmonic solution can be easily restarted from a converged steady one, the overall cost of the nonlinear harmonic solution is about 5 times of a standard steady mixing-plane solution. Compared to multi-passage/whole annulus URANS which can be by three orders of magnitude more costly than the steady-mixing plane solution, the nonlinear harmonic approach should provide two orders of magnitude speed-up. By comparison, the time-spectral/harmonic balance methods tend to be computationally more demanding, especially for multi-disturbances where substantially more sampling points/solutions may be needed to mitigate harmonic aliasing in the Fourier transform during solution (e.g.[54][61][62]).

In the context of modelling compatibility for aeroelastic and aeroacoustic analyses, it should be noted that the time-linearized unsteady flow methods have been well developed and widely used in designs. We may ask, does any of the nonlinear Fourier models reduce to the time-linearized one when the magnitude of relevant aeroelastic and aeroacoustic disturbances diminishes?

A specific context of interest and relevance is that when solving the time-linearized equations, we directly solve the unsteady perturbations (around a given steady base flow). Similarly for the nonlinear harmonic method, we directly solve the unsteady perturbations (around a time-average

flow). As described earlier, Fourier transform is not needed during a nonlinear harmonic solution process. This is in clear contrast to the fully nonlinear solutions (including the time-spectral/'harmonic balance' solutions), where the full flow variables (instead of the unsteady perturbations) are solved. More relevantly unsteady disturbance perturbations can only be worked out by taking differences between full flow variables when the Discrete Fourier transform is used to produce unsteady harmonics during a solution process. There are thus relatively large numerical errors in these harmonic flow variables when unsteady disturbances become very small, simply because small differences between very large numbers in the DFT lead to large errors. In terms of numerical accuracy, a solution of a time-linearized equation can thus be effectively of one order higher accuracy compared to its fully nonlinear counterpart with the same discretization scheme. Hence the time-linearized methods are strongly preferred in prediction of aero-acoustic propagation, where the magnitude of meaningful unsteady pressure disturbances (acoustic signals) can be by 3-4 orders of magnitude smaller than that of the mean pressures.

Hence, the nonlinear harmonic formulation does provide the modelling consistency. When unsteady disturbances become very small, the corresponding time-averaged equations will reduce to the full steady ones, and the nonlinear harmonic equations will reduce to the fully time-linearized harmonic ones, capable of capturing and resolving accurately those small unsteady disturbances of relevance. It is recognized that the baseline nonlinear harmonic method [40-42] does involve extra truncations of the harmonic cross-coupling terms, and thus will probably be more suitable for relatively small disturbance magnitudes in a range from a completely linear regime to a moderately nonlinear one. The time spectral ('harmonic balance') type of models, on the other hand, should be better placed to handle much stronger nonlinearity, when required.

Closing Remarks

There has been a continuous need to develop efficient and accurate prediction methods for turbomachinery blade design, research and development. The Fourier modelling in truncated temporal and/or spatial domains provides a very useful approach to efficient simulations and analysis of effects of nonlinear disturbances on turbomachinery flows. In this lecture the principal modelling aspects pertinent to the method development are introduced. A number of versatile forms and options of the developed methods are presented with examples illustrating the main application capabilities. The Fourier model, by its very nature, is a truncated (reduced) model, which does not solve all the length scales as a direct method does (mesh-resolution permitting). The overriding consideration is a clear appreciation of the relevant length scales for the problems to be solved. The filtering (truncating) ability of a Fourier model should be regarded a strength rather than a weakness for solving practical turbomachinery problems. The past 35 years have witnessed a huge increase in computer power. During the same time period there has been a significant progress in the development of Fourier methods for various turbomachinery applications, which has effectively become part of the turbomachinery CFD ecosystem. Further development and applications of truncated/reduced methods aided by physical insight and computational modelling understanding are expected.

References

1. He, L., 2010 "Fourier Methods for Turbomachinery Applications". Progress in Aerospace Sciences, Vol.46, Issue 8.

2. Smith L.H., 1966 "The Radial-Equilibrium Equation of Turbomachinery". ASME Journal of Engineering for Power, Vol. 88, pp1-22.
3. Marsh, H., 1966 "A Digital Computer Program for the Through-flow Fluid Mechanics in an Arbitrary Turbomachine in a Matrix Method". ARC R&M 3509.
4. Wu, C.H., 1952 "A General Theory of Three-Dimensional Flow in Subsonic or Supersonic Turbomachines of Axial-, Radial- and Mixed-Flow Type," NACA TN 2604.
5. Denton, J.D., 1975 "A time marching method for two and three dimensional blade to blade flows". ARC R&M 3775.
6. Denton J. D. and Prince D.C. Jr., 1983 "An improved time-marching method for turbomachinery flow calculation". Journal of Engineering for Power, Vol. 105, No.3.
7. Denton, J.D., 1992 "The calculation of three-dimensional viscous flow through multistage turbomachine". ASME Journal of Turbomachinery, Vol. 114, No. 1.
8. Dawes, WN, 1988, "Development of a 3D Navier-Stokes solver for application to all types of turbomachinery." ASME Paper No. 88-GT-70.
9. Dawes, W.N., 1992 "Toward improved throughflow capability: the use of three-dimensional viscous flow solvers in a multistage environment". Journal of Turbomachinery, Vol 114, No.1.
10. Hah, C., 1987 "Calculation of three-dimensional viscous flows in turbomachinery with an implicit relaxation method". Journal of Propulsion and Power. Vol. 3, No.5.
11. Arnone, A., 1994 "Viscous analysis of 3-d rotor flow using a multigrid method". Journal of Turbomachinery., Vol. 116, No.3.
12. Gerolymos, G.A, Neubauer, J., Sharma, VC, Vallet I., 2002 "Improved prediction of turbomachinery flows using near-wall Reynolds-stress model". J. Turbomach, Vol. 124, No.1.
13. Denton, JD, and Singh, U.K., 1979 "Time-marching methods for turbomachinery flow calculations", VKI –LEC-SER-1979-7, von Karman Inst for Fluid Dynamics, Belgium.
14. Adamczyk. J.J., 1985 "Model equations for simulating flows in multistage turbomachinery". ASME Paper 85-GT-226.
15. Jameson, A., 1991 "Time-dependent calculations using multigrid, with applications to unsteady flows past airfoil and wings". AIAA paper 91-1596.
16. Lane, F. 1956, "System mode shapes in flutter of compressor blade rows". Journal of the Aeronautical Sciences, Vol.23, No.1.
17. Whitehead, D.S., 1962 "Force and moment coefficients for vibrating aerofoils in cascade". A.R.C. R&M Report No.3254.
18. Atassi, H, and Akai, T.J. 1978 "Aerodynamics force and moment in oscillating aerofoils in cascade". ASME Paper 78-GT-181.
19. Adamczyk, J. J., and Goldstein M.E., 1978 "Unsteady flow in a supersonic cascade with leading-edge locus". AIAA J. Vol.16., No12.
20. Ni, R H. and Sisto, F. 1975, "Numerical computation of nonstationary aerodynamics of flat plate cascade in compressible flow". ASME Paper, 75-GT-5.
21. Whitehead, D S, 1982 "The calculations of steady and unsteady transonic flow in cascades", Report CUED/A-Turbo/TR118, Cambridge University Engineering Department.
22. Verdon, JM, and Caspar, J.R., 1982 "Development of a linear unsteady aerodynamics for finite-deflection cascades". AIAA J., Vol.20, No.9.
23. Hall, KC. and Crawley, E.F., 1989 "Calculation of unsteady flows in turbomachinery using the

linearized Euler equations", AIAA Journal, Vol. 27, No.6.

24. Hall, KC, and Lorence, CB, 1993 "Calculation of three dimensional unsteady flows in turbomachinery using the linearized harmonic Euler equations", ASME J. of Turbomachinery, Vol.115, No.4.
25. Clark, WS. and Hall, KC., 2000 "A time-linearised Navier-Stokes analysis of stall flutter", ASME J. of Turbomachinery, Vol.122., No.3.
26. Sbardella, L. and Imregun, M., 2001 "Linearised unsteady viscous turbomachinery flows on hybrid grids", ASME Journal of Turbomachinery, Vol. 123, No.3.
27. He, L., 2003, "Unsteady flow and aeroelasticity". Chapter 5, Handbook of Turbomachinery, 2nd edition. edited by Logon E Jr, Roy R. Marcel Dekker, Inc.
28. He, L., 1989 "An Euler solution for unsteady flows around oscillating blades". ASME Paper 89-GT-279; also, ASME Journal of Turbomachinery, Vol.112, No.4, 1990.
29. Erdos, J.I., Alzner, E., and McNally, W., 1977 "Numerical Solution of Periodic Transonic Flow through a Fan Stage". AIAA Journal, Vol.15, No.11.
30. He, L., 1992 "A Method of Simulating Unsteady Turbomachinery Flows with Multiple Perturbations". AIAA Journal, Vol.30, No.12.
31. Dewhurst, S, He, L., 2000 "Unsteady flow calculations through turbomachinery stages using single-passage domain with shape-correction method". Proc of the 9th International Symposium on Unsteady Aerodynamics and Aeroelasticity in Turbomachines, Lyon, France.
32. Burgos, M.A. and Corral, R., 2001 "Applications of phase-lagged boundary conditions to rotor-stator interaction". ASME Paper, 2001-0586.
33. Schnell, R., 2004 "Investigation of the tonal acoustic field of a transonic fan stage by time-domain CFD calculations with arbitrary blade counts", ASME Paper, GT-2004-54216.
34. Li, H.D., and He, L., 2002 "Single-passage analysis of unsteady flows around vibrating blades of a transonic fan under inlet distortion". ASME Journal of Turbomachinery, Vol.124, No.2.
35. Li, H.D., and He, L., 2005 "Towards intra-row gap optimization for 1&1/2 stage transonic compressor", ASME Journal of Turbomachinery, Vol.127, No.3, pp589-598.
36. Stapelfeldt, S. C., Parry T, Vahdati, M, 2015 "Validation of time-domain single-passage methods for the unsteady simulation of a contra-rotating open rotor", Proc IMechE, Part A, J. of Power and Energy, Vol.229, No.5. 2015.
37. Stapelfeldt, S. C. and Di Mare L, 2015 "Reduced Passage Method for Multirow Forced Response Computations", AIAA J , Vol.53, No.10.
38. Gerolymos, GA. Michon, GJ, Neubauer, J., 2002 "Analysis and application of chorochronic periodicity in turbomachinery rotor/stator interaction computations". Journal of Propulsion and Power, Vol.18, No.5.
39. Giles, MB, 1992 "An approach for multi-stage calculations incorporating unsteadiness", ASME Paper 92-GT-282.
40. He, L., 1996 "Modelling issues for time-marching calculations of unsteady flows, blade row interaction and blade flutter", VKI Lecture Series: Unsteady Flows in Turbomachines, von Karman Institute for Fluid Dynamics.
41. He, L, and Ning, W., 1998 "Efficient approach for analysis of unsteady viscous flows in turbomachines", AIAA Journal, Vol.36, No.11, pp.2005-2012.

42. Ning, W, and He, L. 1998 "Computation of unsteady flows around oscillating blades using linear and non-linear harmonic Euler methods", Journal of Turbomachinery, Vol.120, No.3.
43. Chen, T., Vasanthakumar P, and He, L., 2001 "Analysis of unsteady blade row interaction using nonlinear harmonic approach". Journal of Power and Propulsion, Vol. 17. No.3.
44. He, L., Chen, T., Wells, R.G., Li, Y.S., & Ning, W., 2002 "Analysis of rotor-rotor and stator-stator interferences in multi-stage turbomachines". J. of Turbomachinery, Vol.124, No.4.
45. Hall, K.C., Thomas, J.P., and Clark, W.S., 2000 "Computation of unsteady nonlinear flows in cascades using a harmonic balance technique". Presented at 9th international symposium on unsteady aerodynamics, aeroacoustics and aeroelasticity of turbomachines, Lyon, France.
46. Hall, K.C., Thomas J.P. and Clark WS, 2002 "Computation of unsteady nonlinear flows in cascades using a harmonic balance technique", AIAA Journal, Vol.40, No.5.
47. McMullen M, Jameson A, Alonso J.J., 2001 "Acceleration of convergence to a periodic steady state in turbomachinery flows". AIAA Paper 2001-0152.
48. McMullen M, Jameson A, Alonso J.J., 2002 "Application of a non-linear frequency domain solver to the Euler and Navier-stokes equations". AIAA Paper 2002-0120.
49. McMullen M, Jameson, A, Alonso J.J., 2006 "Demonstration of nonlinear frequency domain methods". AIAA Journal, Vol. 44, No.7.
50. McMullen MS, Jameson, A., 2006 "The computational efficiency of non-linear frequency domain methods". Journal of Computational Physics, Vol.212, Issue 2.
51. Maple. RC, King P, Orkwis, P, Wolff, J.M., 2004 "Adaptive harmonic balance method for nonlinear time-periodic flows". Journal of Computational Physics Vol. 193, No.2.
52. van der Weide E, Gopinath, Jameson A., 2005 "Turbomachinery applications with the time spectral method". AIAA Paper 2005-4905.
53. Gopinath, A, van der Weide E, Alonso, J.J., Jameson A, Ekici, K, and Hall K.C., 2007 "Three-dimensional unsteady multi-stage turbomachinery simulations using the harmonic balance technique". AIAA Paper 2007-0892.
54. Ekici, K., and Hall, K.C., 2007 "Nonlinear analysis of unsteady flows in multistage turbomachines using harmonic balance". AIAA Journal, Vol. 45, No.5.
55. Ekici K, and Hall KC., 2008, "Nonlinear frequency-domain analysis of unsteady flows in turbomachinery with multiple excitation frequencies". AIAA Journal, Vol.46, No.8.
56. Spiker MA, Kielb RE, Hall KC., 2008 "Efficient design method for non-synchronous vibrations using enforced motion", ASME Paper GT2008-50599.
57. Sicot, F., Guédeney, T, Guillaume Dufour G, 2013 "Time-domain harmonic balance method for aerodynamic and aeroelastic simulations of turbomachinery flows", International Journal of Computational Fluid Dynamics, Vol.27, No.2.
58. Frey, C., Ashcroft, G., Kersken, H-P, and Voigt, C., 2014 "A Harmonic Balance Technique for Multistage Turbomachinery Application", ASME Paper GT2014-2523.
59. Wang D.X. and Huang, X. Q., 2017 "A complete rotor–stator coupling method for frequency domain analysis of turbomachinery unsteady flow". Aerospace Science and Technology, Vol.70, pp 367-377.
60. Huang X Q, and Wang, D.X., 2019 "Time-Space Spectral Method for Rotor–Rotor/Stator–Stator Interactions". Journal of Turbomachinery, Vol.141 (11).
61. Junge, L., Frey, C., Ashcroft, G., and Kügeler, E., 2021 "A New Harmonic Balance Approach

Using Multidimensional Time,", ASME J. Eng. Gas. Turbines. Power, Vol.143(8).
62. Wang D.X., Zhang S, 2022 "An Approximate Time Domain Nonlinear Harmonic Method for Analysing Unsteady Flows with Multiple Fundamental Modes", J. Turbomach., Vol.144(12).
63. Wu, L., Du, P.C., and Ning, F. F., 2025 "Validation of the time-space collocation method in simulating the inlet distortion flows in transonic compressor." Journal of the Global Power and Propulsion Society. Vol.9, pp58-76.
64. Romagnosi L., Li Y., Mezine M., Teixeira M., Vilmin S., Anker, J.E., Claramunt, K., Baux, Y., and Hirsch, Ch, 2019 "A Methodology for Steady and Unsteady Full-engine Simulations", ASME Paper GT2019-90110.
65. Vilmin S, Lorrain E , Hirsch C, Swoboda M, 2006 "Unsteady flow modeling across the rotor/stator interface using the nonlinear harmonic method". ASME Paper GT2006-90210.
66. Vilmin S, Lorrain E, and Hirsch Ch. 2009 "Application of a nonlinear harmonic method to the simulation of clocking effects". ASME Paper, GT2009-59475.
67. He, L., 2006 "Fourier modelling of Nonaxisymmetrical Steady and Unsteady Flow", Journal of Propulsion and Power, Vol.22, No.1.
68. Romero, D. and Corral R, 2020 "Impact of downstream potential perturbations on the nonlinear stability of a generic fan". J. of Global Power and Propulsion Society. Vol.4, pp217-225.
69. Corral R, Romero, D. and Montiel M., 2024 "Block Spectral Method Analysis for Turbomachinery Applications". ASME J. of Turbomachinery, Vol.146(7).
70. He, L., 2011 "Efficient computational model for non-axisymmetric flow and heat transfer in rotating cavity". ASME J. of Turbomachinery, Vol.133(2).
71. Romero, D. and Corral R., 2021 "Nonlinear Stability Analysis of a Generic Fan with Distorted Inflow Using Passage-Spectral Method", ASME J. of Turbomachinery, Vol.143(6).
72. He, L., 2013 "Fourier Spectral Method for Multi-scale Aerothermal Analysis", International Journal of Computational Fluid Dynamics, Vol.27, No.2.
73. Owen, J.M., 2010 "Thermodynamic analysis of buoyancy-induced flow in rotating cavities", Journal of Turbomachinery, Vol.132, No.3, 031006.
74. Bohn, D. Ren, J. and Tuemmers, C., 2006 "Investigation of the unstable flow structure in a rotating cavity", ASME Paper GT2006-90494.
75. Vasanthakumar P., 2003, "Three-dimensional frequency-domain solution method for unsteady turbomachinery flows". PhD Thesis, Durham University, Durham, UK.
76. Holmes D.G., Mitchell, BE, Lorence, CB, 1997 "Three-dimensional linearized Navier-Stokes calculations for flutter and forced response", Proc of 8th International Symposium on Unsteady Aerodynamics and Aeroelasticity of Turbomachines, Ed. Fransson, TH, Stockholm, Sweden.
77. He, L., 2008 "Harmonic solution of unsteady flow around blade with separation", AIAA Journal, Vol.46, No.6.
78. Wang, D. X., and He, L., 2009 "Concurrent Aerodynamic-Aeromechanic Design Optimization for Turbomachinery Blades Using Adjoint Method", ASME Paper GT2009-59240.
79. He, L., and Wang, D. X., 2011 "Concurrent Aerodynamic-Aeroelastic Design Optimization using Adjoint Method", ASME Journal of Turbomachinery, Vol.133. No.1.
80. Wang, D. X., He, L., Li, Y.S., Chen T. and Wells, R.G., 2010 "Adjoint Aerodynamic Design Optimization for Blades in Multi-Stage Turbomachines: Part II–Verification and Application", ASME Journal of Turbomachinery, Vol.132, No.2, 021012.